GS-9219—A Novel Acyclic Nucleotide Analogue with Potent Antineoplastic Activity in Dogs with Spontaneous Non–Hodgkin's Lymphoma

Hans Reiser,[1] Jianying Wang,[1] Lee Chong,[1] William J. Watkins,[1] Adrian S. Ray,[1] Riri Shibata,[1] Gabriel Birkus,[1] Tomas Cihlar,[1] Sylvia Wu,[1] Bei Li,[1] Xiaohong Liu,[1] Ilana N. Henne,[1] Grushenka H.I. Wolfgang,[1] Manoj Desai,[1] Gerald R. Rhodes,[1] Arnold Fridland,[1] William A. Lee,[1] William Plunkett,[2] David Vail,[3,4] Douglas H. Thamm,[5] Robert Jeraj,[4] and Daniel B. Tumas[1]

Abstract

Purpose: GS-9219, a novel prodrug of the nucleotide analogue 9-(2-phosphonylmethoxyethyl)guanine (PMEG), was designed as a cytotoxic agent that preferentially targets lymphoid cells. Our objective was to characterize the antiproliferative activity, pharmacokinetics, pharmacodynamics, and safety of GS-9219.

Experimental Design: GS-9219 was selected through screening in proliferation assays and through pharmacokinetic screening. The activation pathway of GS-9219 was characterized in lymphocytes, and its cytotoxic activity was evaluated against a panel of hematopoietic and nonhematopoietic cell types. To test whether the prodrug moieties present in GS-9219 confer an advantage over PMEG *in vivo*, the pharmacokinetics, pharmacodynamics (lymph node germinal center depletion), and toxicity of equimolar doses of GS-9219 and PMEG were evaluated after i.v. administration to normal beagle dogs. Finally, proof of concept of the antitumor efficacy of GS-9219 was evaluated in five pet dogs with spontaneous, advanced-stage non–Hodgkin's lymphoma (NHL) following a single i.v. administration of GS-9219 as monotherapy.

Results: In lymphocytes, GS-9219 is converted to its active metabolite, PMEG diphosphate, via enzymatic hydrolysis, deamination, and phosphorylation. GS-9219 has substantial antiproliferative activity against activated lymphocytes and hematopoietic tumor cell lines. In contrast, resting lymphocytes and solid tumor lines were less sensitive to GS-9219. GS-9219, but not PMEG, depleted the germinal centers in lymphoid tissues of normal beagle dogs at doses that were tolerated. In addition, GS-9219 displayed significant *in vivo* efficacy in five dogs with spontaneous NHL after a single administration, with either no or low-grade adverse events.

Conclusion: GS-9219 may have utility for the treatment of NHL.

Authors' Affiliations: [1]Department of Research and Development, Gilead Sciences, Inc., Foster City, California; [2]Department of Experimental Therapeutics, M. D. Anderson Cancer Center, Houston, Texas; [3]Center for Clinical Trials and Research, School of Veterinary Medicine and [4]Paul P. Carbone Comprehensive Cancer Center, University of Wisconsin, Madison, Wisconsin; and [5]College of Veterinary Medicine and Biomedical Sciences, Colorado State University, Fort Collins, Colorado

Received 8/21/07; revised 11/16/07; accepted 12/13/07.

Grant support: Gilead Sciences, Inc.

The costs of publication of this article were defrayed in part by the payment of page charges. This article must therefore be hereby marked *advertisement* in accordance with 18 U.S.C. Section 1734 solely to indicate this fact.

Note: Supplementary data for this article are available at Clinical Cancer Research Online (http://clincancerres.aacrjournals.org/).

Conflict of interest: H. Reiser, J. Wang, W.J. Watkins, A.S. Ray, R. Shibata, G. Birkus, T. Cihlar, S. Wu, B. Li, X. Liu, I.N. Henne, G.H.I. Wolfgang, M. Desai, G.R. Rhodes, A. Fridland, W.A. Lee, and D.B. Tumas are employees and/or shareholders of Gilead Sciences, Inc.

Requests for reprints: Hans Reiser, Department of Research and Development, Gilead Sciences, Inc., 333 Lakeside Drive, Foster City, CA 94404. Phone: 650-522-6327; E-mail: hans.reiser@gilead.com.

doi:10.1158/1078-0432.CCR-07-2061

Non–Hodgkin's lymphoma (NHL) is the second fastest growing form of cancer and the fifth leading cause of cancer deaths in the United States. The American Cancer Society estimates that the annual incidence of all forms of NHL in the United States in 2006 was 58,870 cases. In 2006, the estimated number of deaths due to NHL in the United States was 18,840 (1). Despite the introduction of rituximab in 1997, the latest Surveillance Epidemiology and End Results 5-year relative survival data (1999-2003) show a 5-year survival rate of 63% in NHL (indolent NHL ranges from 71% to 89%, depending on subtype; aggressive NHL ranges from 34% to 54%; ref. 1). Therefore, there is still a major unmet medical need in NHL patients for novel agents with improved efficacy compared with existing treatment modalities, especially in NHL patients who have failed frontline therapy.

The acyclic nucleotide 9-(2-phosphonylmethoxyethyl)guanine (PMEG) forms an active phosphorylated metabolite, PMEG diphosphate (PMEGpp), in cells and causes cytotoxicity in dividing cells due to potent inhibition of the nuclear DNA polymerases α, δ, and ε, resulting in inhibition of DNA

synthesis and/or DNA repair (2). In rodent models, PMEG has activity against leukemia and melanoma. However, the utility of PMEG as an anticancer agent is limited by its poor cellular permeability and toxicity, especially for the kidney and gastrointestinal tract (3–5).

We synthesized prodrug analogues of PMEG to improve permeability and selectivity, with the hypothesis that this would lead to better efficacy and a more favorable therapeutic window. As lymphoid malignancies were the primary target of this effort, our strategy was to identify a PMEG prodrug that effectively loaded peripheral blood mononuclear cells (PBMC) with PMEGpp and resulted in minimal plasma levels of PMEG. Compounds were analyzed for their antiproliferative activity *in vitro* and for their cell and tissue distribution *in vivo* following i.v. administration. As a starting point for prodrug design, we used the N^6-substituted prodrug of PMEG, 9-(2-phosphonylmethoxyethyl)-N^6-cyclopropyl-2,6-diaminopurine (cPrPMEDAP), due to its specific intracellular activation and ability to limit plasma exposure to the nephrotoxic agent PMEG (6, 7). Phosphonoamidate prodrug moieties were added to increase the efficiency of lymphoid cell and tissue loading. Here, we describe a novel compound, GS-9219 (diethyl *N,N′*-[({2-[2-amino-6-(cyclopropylamino)-9*H*-purin-9-yl]ethoxy}methyl)phosphonoyl]di-L-alaninate), which met the pharmacokinetic and potency selection criteria. The cytotoxic activity of GS-9219 was evaluated *in vitro* against a panel of hematopoietic and nonhematopoietic cell lines. To test whether the prodrug moieties present in GS-9219 confer an advantage over PMEG *in vivo*, the pharmacokinetics, pharmacodynamics (lymph node germinal center depletion), and toxicity of equimolar doses of GS-9219 and PMEG were evaluated after i.v. administration to normal beagle dogs. Finally, proof of concept of the antitumor efficacy of GS-9219 was evaluated in five pet dogs with naturally occurring, advanced-stage NHL following a single i.v. administration of GS-9219 as monotherapy.

Materials and Methods

Compounds. GS-9219 (succinate salt), cPrPMEDAP, PMEG, PMEGp, PMEGpp, and 9-(2-phosphonomethoxyethyl)-2,6-diaminopurine (PMEDAP) were synthesized at Gilead Sciences, Inc. Cytarabine, cladribine, and fludarabine desphosphate were purchased from Sigma. Clofarabine was synthesized by Acme Biosciences. Deoxycoformycin was purchased from SuperGen.

Cell culture and proliferation assays. All cell lines were purchased from the American Type Culture Collection and cultured in RPMI 1640 (Life Technologies/Invitrogen) supplemented with 15% fetal bovine serum (Hyclone), 2 mmol/L L-glutamine (Life Technologies/Invitrogen), and antibiotics. PBMCs were isolated by Ficoll-Hypaque density gradient centrifugation using standard procedures. T and B cells were purified using antibody-conjugated magnetic beads. T lymphoblasts were generated by stimulation of $CD3^+$ T cells with 1 μg/mL phytohemagglutinin (PHA-P; Sigma) and 10 units/mL interleukin-2 (Roche Applied Science; ref. 8). B lymphoblasts were generated by stimulation of $CD19^+$ B cells with 20 μg/mL pokeweed mitogen (Sigma). Cell proliferation was quantified either by bromodeoxyuridine (BrdUrd) incorporation assay or by 2,3-bis[2-methoxy-4-nitro-5-sulfophenyl]-2H-tetrazolium-5-carboxanilide inner salt (XTT) assay (Roche Diagnostics).

Metabolite analysis following in vitro cell loading with [^{14}C]GS-9219. Twenty million PHA-stimulated T cells were incubated with 10 μmol/L [^{14}C]GS-9219 for 24 h. Cells were washed once with tissue culture medium and twice with PBS, incubated in 80% methanol overnight, and centrifuged at 14,000 rpm for 15 min to remove denatured proteins. The methanol extracts were lyophilized and dissolved in the high-performance liquid chromatography (HPLC) loading buffer. A portion of each sample was used for scintillation counting to calculate the total pmoles, and the rest was used for HPLC analysis to calculate the ratio of metabolites. HPLC analysis was done by gradient elution using a Phenomenex Prodigy column (5 μm, ODS3 150 × 4 mm), where buffer A is 25 mmol/L K_2HPO_4 (pH 6.0) and 5 mmol/L tetrabutylammonium bromide and buffer B is 25 mmol/L K_2HPO_4 (pH 6.0), 70% acetonitrile, and 5 mmol/L tetrabutylammonium bromide.

Pharmacokinetic studies. The plasma and PBMC pharmacokinetic profiles of GS-9219 and select metabolites were determined following a 30-min i.v. infusion of 3 mg/kg GS-9219 (formulated as a 5% dextrose solution) to three male beagle dogs. At predefined time points, blood was drawn for plasma and PBMC isolation. Isolated PBMCs were resuspended in PBS. A small aliquot of cells was used for cell counting to determine the concentration of cells. The remaining cell suspension was centrifuged to pellet cells and the pellet was resuspended in 70% methanol lyses buffer. Plasma levels of GS-9219 and cPrPMEDAP, or PBMC levels of cPrPMEDAP were determined by reverse-phase liquid chromatography using 0.2% formic acid, an acetonitrile gradient, and a Synergi Fusion-RP 80A column (150 × 2.1 mm, 4 μm) or a Synergi Hydro-RP 80A column (50 × 2 mm, 4 μm), respectively (columns purchased from Phenomenex, Inc.). Detection of analytes was accomplished by mass spectrometry using an API 4000 triple quadruple instrument (Applied Biosystems/MDS Sciex) operating in multiple reaction monitoring and positive ionization modes. PBMC samples were analyzed for PMEGpp using ion pairing liquid chromatography coupled to positive mode mass spectrometry essentially as described previously for other analytes (9). The tissue distribution of [^{14}C]GS-9219 and [^{14}C]PMEG (5-10 μCi/kg) were determined 24 h following 30-min i.v. infusions to male beagle dogs. Total radioactivity levels in PBMCs, lymph nodes (sum of levels in the axillary, iliac, inguinal, and mesenteric nodes), liver, and kidney are reported. Metabolite identification was done on liver and kidney tissues 24 h following administration of radiolabeled GS-9219. Metabolites were identified based on the retention of radiolabeled peaks relative to authentic standards.

Comparative safety evaluation of GS-9219 and PMEG in normal beagle dogs. Safety evaluation of GS-9219 and PMEG in male beagle dogs, 7 to 9 mo of age, was done at contract laboratories (Covance Laboratories, Inc. and MPI Research, Inc.) in compliance with the Animal Welfare Act, the Guide for the Care and Use of Laboratory Animals, and the Office of Laboratory Animal Welfare. Three animals were used per dose group. PMEG (0.25 mg/kg), GS-9219 (0.3 or 0.5 mg/kg), or the vehicle (5% dextrose for injection; U.S. Pharmacopeia) was given daily by 30-min i.v. infusion. Animals were evaluated clinically twice daily and routine hematology, clinical chemistry, and urinalysis were evaluated twice before treatment, on days 1 and 2, and 24 h after the last dose. Plasma samples for pharmacokinetics were attained at approximately 0.5, 1, 2, 4, 6, 8, and 24 h after the initiation of infusion on the first and last day of treatment. After an overnight fast, animals were euthanized 24 h after the last dose with sodium pentobarbital solution and evaluated by gross and microscopic examination.

Efficacy evaluation of GS-9219 in dogs with NHL. Pet owners presenting to the School of Veterinary Medicine, University of Wisconsin-Madison (Madison, WI) or the College of Veterinary Medicine and Biomedical Sciences, Colorado State University (Fort Collins, CO) were offered entry into this study for treatment of their dogs with GS-9219 under compliance with the Animal Care and Use Committees of the University of Wisconsin-Madison and Colorado State University, and the Clinical Review Board of the Colorado State University Veterinary Medical Center. Dogs were evaluated by complete physical examination, routine clinical chemistry, hematology and urinalysis, and diagnostic lymph node biopsy inclusive of histology and immunohistochemistry to confirm NHL and determine

immunophenotype. Concurrent antineoplastic therapy was not allowed. Previous cytotoxic chemotherapy was allowable, with a 3-wk washout from the most recent treatment. Toxicity was graded according to the Veterinary Cooperative Oncology Group Common Terminology Criteria for Adverse Events v1.0, modified from the National Cancer Institute Common Terminology Criteria for Adverse Events used in humans (10), based on client questionnaire, physical examination, complete blood count, biochemistry profile, and urinalysis. Toxicity evaluations were done before treatment and on two occasions within the first 2 wk after treatment. GS-9219 was given at 1 mg/kg (0.82 mg/kg based on the free base) by a 30-min i.v. infusion in 5% dextrose for injection (2 mL/kg). Efficacy was determined by evaluation of the summation of longest diameter of affected peripheral nodes using Response Evaluation Criteria in Solid Tumors criteria for the pretreatment and posttreatment (5-7 d after infusion with GS-9219) measurements. One dog was additionally evaluated by 3′-deoxy-3′-[^{18}F]fluorothymidine-positron emission tomography (FLT-PET) before and after treatment. FLT is a novel marker for imaging tumor cell proliferation *in vivo*. Because the fluorine in FLT is placed in the 3′ position in deoxyribose, FLT works as a terminator of the growing DNA chain. Therefore, little FLT is actually accumulated in DNA, but it is retained intracellularly after phosphorylation by thymidine kinase 1. Direct correlation between FLT uptake and proliferation Ki-67 labeling index has been observed in preclinical and clinical studies. The FLT-PET imaging studies were done on the clinical GE Discovery LS PET/computed tomography (CT) scanner at the University of Wisconsin Hospitals and Clinics. FLT was obtained from the cyclotron and radiopharmaceutical laboratory at the Department of Medical Physics at the University of Wisconsin-Madison. FLT activity

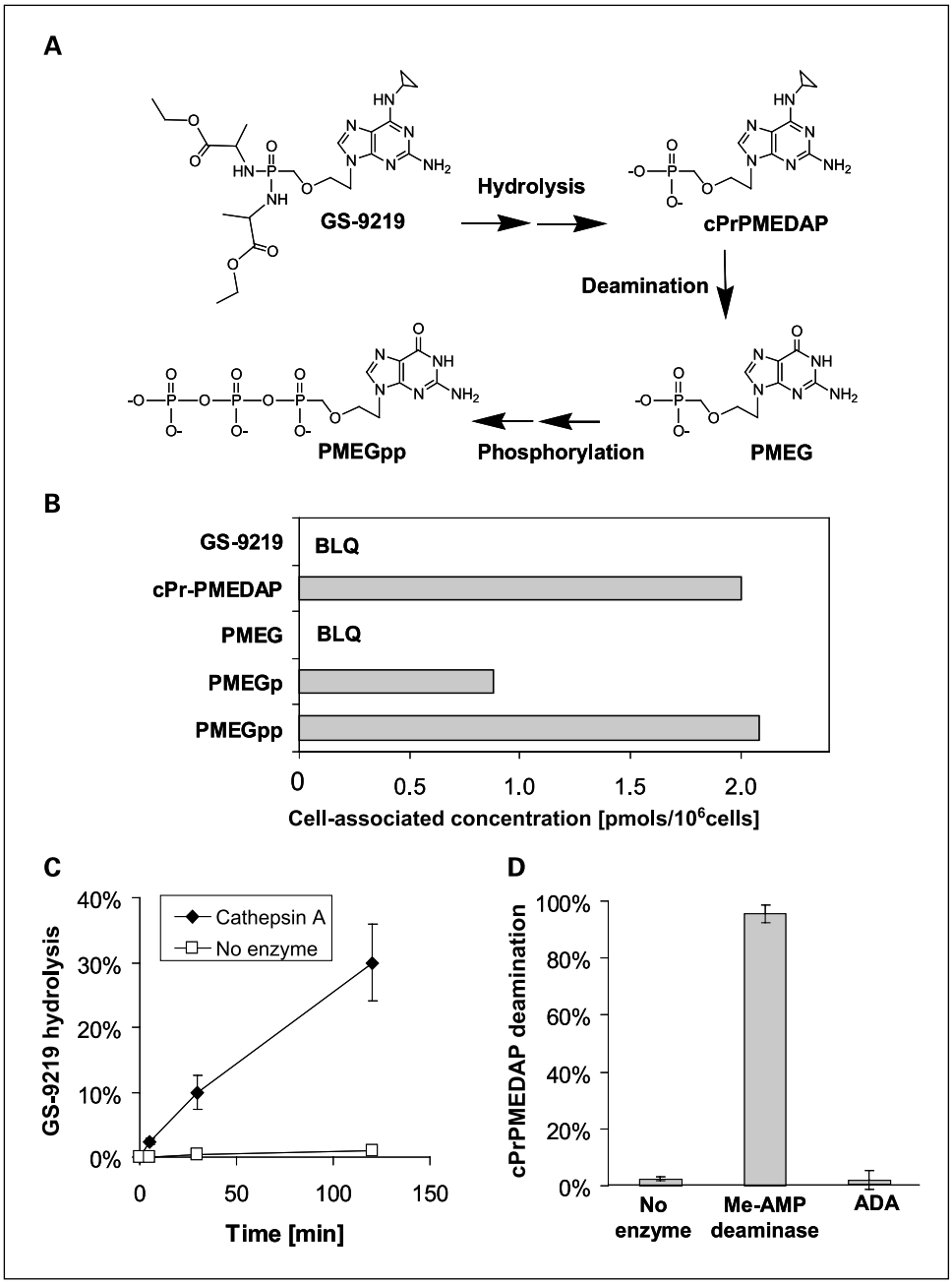

Fig. 1. Metabolic conversion of GS-9219 to PMEGpp. *A,* proposed intracellular pathway. *B,* concentrations of GS-9219 metabolites in activated T cells. PHA-stimulated T cells were incubated with [^{14}C]GS-9219 and cell lysates were prepared as detailed in Materials and Methods. Indicated are mean values of compounds/metabolites in pmol/10^6 cells. BLQ, concentrations below the limit of quantification. *C,* hydrolysis of GS-9219 by cathepsin A. GS-9219 (30 μmol/L) was incubated in reaction buffer [25 mmol/L Na-MES (pH 6.5), 100 mmol/L NaCl, 1 mmol/L DTT, 0.1% NP40] in the presence and absence of 0.15 μg/mL cathepsin A. Percent hydrolysis of GS-9219 at 5, 30, and 120 min was quantified by reverse-phase HPLC. *D,* deamination of cPrPMEDAP. [^{3}H]cPrPMEDAP was incubated in K-HEPES buffer (pH 7.5) in the absence of enzyme and in the presence of 10 μg/mL N^6-methyl-AMP aminohydrolase or 200 μg/mL adenosine deaminase. After a 30-min incubation, percent conversion of cPrPMEDAP to PMEG was quantified by radiometric HPLC.

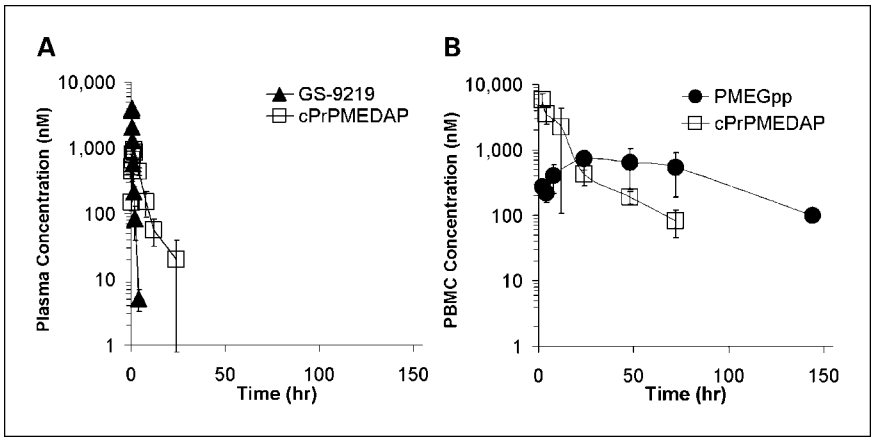

Fig. 2. Selective delivery of PMEGpp to lymphoid cells by GS-9219 in the absence of detectable plasma exposure to PMEG. The plasma (*A*) and PBMC (*B*) pharmacokinetic profiles of GS-9219 (▲), cPrPMEDAP (□), and PMEGpp (●) were characterized in normal beagle dogs following a 30-min i.v. infusion of 3 mg/kg GS-9219. Data points, mean of results obtained from three animals; bars, SD.

(5 mCi, 185 MBq) was given per scan. The whole-body FLT-PET image acquisition with 10-min scan per bed position was initiated after 60 ± 10 min after injection. For this study, the body mass standardized uptake values were calculated.

Results

Intracellular metabolism of GS-9219. GS-9219 (Fig. 1A) was selected from a library of cPrPMEDAP prodrugs through pharmacokinetic screening in normal beagle dogs. For this purpose, compounds were given at low doses by i.v. infusion, and the concentrations of the metabolites, cPrPMEDAP and PMEGpp, were measured in PBMCs and plasma over a period of 24 h following the end of infusion. A high ratio of intracellular to plasma concentration of GS-9219 metabolites indicated that GS-9219 is efficiently taken up by PBMCs and metabolized.

The formation of GS-9219 metabolites was examined in PHA-stimulated human T cells from six normal donors after 24-h treatment with 10 μmol/L [^{14}C]GS-9219. The major metabolites were cPrPMEDAP, PMEGp, and PMEGpp, whereas GS-9219, PMEG, and monophosphorylated and diphosphorylated metabolites of cPrPMEDAP were either undetectable or too low for accurate quantification (Fig. 1B). Experiments with canine T cells yielded similar results (data not shown).

We conducted a series of experiments to characterize the enzymes involved in the intracellular activation of GS-9219. Cathepsin A, a lysosomal carboxypeptidase, is the enzyme responsible for the initial hydrolysis of certain antiviral prodrugs of similar structure (11). We therefore tested whether GS-9219 was a substrate for cathepsin A. Whereas the hydrolysis rate of GS-9219 in human PBMC lysates was 0.56 pmol/min*μg (data not shown), purified cathepsin A was able to hydrolyze GS-9219 at a rate of 1,200 pmol/min*μg (Fig. 1C), suggesting a role for this serine protease in the catabolism of GS-9219. Whether there are other intracellular enzymes capable of hydrolyzing GS-9219 is currently unknown. Next, we searched for enzymes capable of deaminating cPrPMEDAP to PMEG, a requisite step in the formation of the active metabolite PMEGpp. cPrPMEDAP bears a structural similarity to N^6-cyclopropyl–substituted abacavir monophosphate, an intermediate in the intracellular metabolism of the antiretroviral nucleoside abacavir that is effectively deaminated to the corresponding guanine analogue by N^6-methyl-AMP aminohydrolase (12). Therefore, we tested the ability of N^6-methyl-AMP aminohydrolase to deaminate cPrPMEDAP. As shown in Fig. 1D, this enzyme was able to deaminate cPrPMEDAP *in vitro*. This reaction is efficiently inhibited by the deaminase inhibitor deoxycoformycin monophosphate (data not shown). We cannot rule out that there are other enzymes

Table 1. Antiproliferative activity of GS-9219 in lymphoblasts and hematopoietic cell lines

Compound	EC_{50} (nmol/L)								
	T-cell blasts	B-cell blasts	CEM	Molt-4	KG-1	HL-60	RL	Daudi	PM-1
GS-9219	135	42	156	27.3	1,043	214	78	27	125
cPrPMEDAP	2,348	—	2,217	1,473	1,109	1,608	—	1,838	6,725
PMEG	1,679	—	5,195	1,739	2,928	3,918	—	994	4,022
PMEDAP	8,953	—	19,874	27,896	7,633	21,667	—	14,405	22,732
Cytarabine	1,820	—	143	23	56	212	610	209	194
Clofarabine	62	126	418	25	60	73	50	221	145
Cladribine	296	—	1,167	74	89	50	4	525	40
Fludarabine	1,102	—	>40,000	1,550	4,518	1,768	—	—	12,857

NOTE: The ability of GS-9219 to inhibit the proliferation of lymphoblasts and cell lines was analyzed in 3-d assays using BrdUrd incorporation to assess proliferation. The following cell lines were tested: CEM, Molt-4, and PM-1 (T cell); RL and Daudi (B cell); and KG-1 and HL-60 (myeloid). All data points represent mean values from at least three independent experiments.

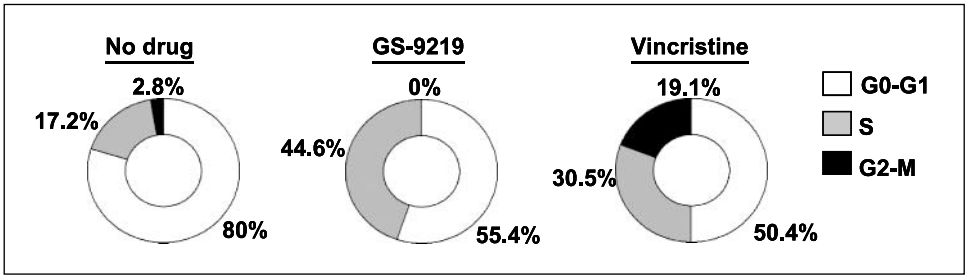

Fig. 3. Induction of cell cycle arrest in the S phase by GS-9219. PHA-stimulated T cells were incubated for 72 h with no compound (*left*), with 20 times EC_{50} concentration of GS-9219 (*middle*), or with 20 times EC_{50} concentration of the mitosis inhibitor vincristine (*right*). The amount of DNA in each nucleus was quantified by propidium iodide staining followed by flow cytometric analysis. Percentage of cells at each cell cycle stage was calculated using ModFit LT software.

capable of deaminating cPrPMEDAP in lymphocytes; however, the ability of adenosine deaminase to deaminate cPrPMEDAP to PMEG is negligible (Fig. 1D).

These findings suggest that the intracellular activation pathway for GS-9219 is as depicted in Fig. 1A. Intracellularly, the bis(Ala-ethyl) prodrug moiety of GS-9219 is hydrolyzed to produce cPrPMEDAP. Subsequently, the cyclopropyl prodrug moiety of cPrPMEDAP is deaminated to produce PMEG, which is then diphosphorylated to generate the pharmacologically active metabolite, PMEGpp. The fact that cPrPMEDAP and PMEGpp are the predominant GS-9219 metabolites in lymphocytes suggests that deamination rather than phosphorylation is the rate-limiting step in these cells.

The plasma and PBMC pharmacokinetics of GS-9219 and select metabolites were studied in detail after a 30-min i.v. infusion to healthy beagle dogs (Fig. 2). Following i.v. infusion, GS-9219 was rapidly eliminated with a terminal half-life of <30 min and an estimated clearance of 2.25 ± 0.23 L/h/kg, which is in excess of liver blood flow. The disappearance of GS-9219 was accompanied by a concomitant increase in plasma and especially PBMC exposure to cPrPMEDAP. Intracellular levels of cPrPMEDAP slowly decreased due to rate-limiting deamination to PMEG and subsequent phosphorylation to the active species PMEGpp. PMEGpp reached a maximal concentration in PBMCs ~24 h after dose and persisted with an apparent terminal half-life of 36.7 ± 6.5 h. Whereas PMEG and its active metabolite were readily detectable in PBMCs, plasma levels of PMEG remained undetectable (<30 nmol/L). The favorable ratio of $(\text{total PMEG})_{PBMC}/(\text{total PMEG})_{Plasma}$ made GS-9219 suitable for further *in vitro* and *in vivo* characterization.

***Antiproliferative activity of GS-9219* in vitro.** The ability of GS-9219 to inhibit the proliferation of activated lymphocytes and of tumor cells of hematopoietic origin was investigated *in vitro*. GS-9219 inhibited the proliferation of mitogen-stimulated T and B lymphocytes with EC_{50} values of 135 and 42 nmol/L, respectively, as determined by BrdUrd incorporation (Table 1). The activity of GS-9219 against T and B lymphoblasts was only minimally affected by human serum or serum proteins (≤3-fold shift), likely reflecting its low protein binding and high stability in nonrodent plasma (data not shown). To compare the activity of GS-9219 in dividing and nondividing cells, the compound was evaluated in these populations using a metabolism-based sodium XTT assay instead of BrdUrd assays. Results from the XTT assay showed a 127-fold difference between the EC_{50} values of GS-9219 in quiescent (EC_{50} = 17.2 μmol/L) and proliferating (EC_{50} = 135 nmol/L) cells. These results indicate a substantial selectivity of GS-9219 toward actively replicating lymphoblasts.

Inhibition of DNA synthesis is known to arrest the cell cycle in the S phase. To assess the effects of GS-9219 on cell cycle progression, cell cycle profiles of primary human T lymphoblasts were examined by DNA staining with propidium iodide and flow cytometry. Consistent with the proposed mechanism of action, treatment with GS-9219 increased the percentage of T lymphoblasts in the S phase of the cell cycle by >2-fold (Fig. 3). Staining with Annexin V showed that a substantial fraction of GS-9219–treated lymphoblasts underwent apoptosis (data not shown).

The ability of GS-9219 to inhibit the proliferation of various cell lines of hematopoietic origin was tested using BrdUrd incorporation assays. GS-9219 exhibited antiproliferative activity against all cell lines evaluated, including both lymphoid and myeloid cell lines. As in the case of normal T and B lymphoblasts, no significant difference was observed between T and B lymphoid tumor cell lines (Table 1). This finding indicated that, unlike another guanosine analogue, nelarabine, which is only effective against T-cell lymphomas (13), GS-9219 may be effective against both T-cell and B-cell malignancies. Several compounds used for the treatment of hematologic malignancies, including cytarabine, clofarabine, cladribine, and fludarabine, were also evaluated; the EC_{50} values of these compounds were generally similar to those obtained for GS-9219 (Table 1; data not shown).

We also analyzed the ability of GS-9219 metabolites, including cPrPMEDAP and PMEG, to inhibit the proliferation of human PHA lymphoblasts and cell lines. In general, GS-9219 was markedly more potent in inhibiting cell proliferation than its metabolites (Table 1). This result illustrates the positive effect that the GS-9219 prodrug moieties have on the cellular permeability and accumulation in lymphoblasts and cell lines of hematopoietic origin. Deoxycoformycin, a nucleoside analogue intracellularly metabolized to its monophosphate form with potent inhibitory effect for N^6-methyl-AMP aminohydrolase (14), reduced the potency of GS-9219 and cPrPMEDAP in a dose-dependent manner as indicated by an increase in EC_{50} values. In contrast, deoxycoformycin did not affect the potency of PMEG (data not shown), which supports the conclusion that GS-9219 is dependent on deamination of cPrPMEDAP as an essential step to form the active species, PMEGpp.

The ability of GS-9219 to inhibit the proliferation of various cell lines of nonhematopoietic origin was also tested using 3-day BrdUrd incorporation assays. GS-9219 had no significant activity (EC_{50} values > 10 μmol/L) against nine different cancer cell lines, representing a variety of tumor types: MDA-MB-231 (breast), ZR-75-1 (breast), HT-29 (colon), COLO 205 (colon), Caki-1 (kidney), A549 (lung), NCI-H23 (lung), SU.86.86

(pancreas), and PNAC-1 (pancreas). Taken together, the data to date suggest that solid tumor cell lines are less sensitive to GS-9219 than cell lines of hematopoietic origin.

Effect of GS-9219 prodrug moiety on tissue distribution in dogs in vivo. To test the central hypothesis of this drug discovery program, we asked whether the prodrug moieties present in GS-9219 confer an advantage over PMEG. For this purpose, we carried out comparative tissue distribution and safety studies in dogs after i.v. infusions of either GS-9219 or PMEG.

To compare the tissue distribution of GS-9219 and PMEG, normal beagle dogs received 30-min infusions of ^{14}C-labeled compounds, and lymphoid and nonlymphoid tissues (e.g., adrenal glands, bone, brain, duodenum, epididymidis, eyes, kidneys, liver, lungs, lymph node, pancreas, PBMCs, prostate, skin, spinal cord, and testes) were harvested 24 h after the infusion. Although in most tissues, including bone marrow, similar (within 2-fold) amounts of PMEG equivalents were present in dogs infused with GS-9219 or PMEG, certain exceptions were observed (Fig. 4A and B). First, GS-9219 more efficiently loaded PBMCs and lymph nodes with >10-fold and >3.7-fold higher levels of total radioactivity 24 h after dose relative to PMEG, respectively. Second, the administration of GS-9219 resulted in 20-fold lower levels of radioactivity in the kidney. Finally, dosing with GS-9219 produced ~4-fold higher levels of total radioactivity in the liver relative to PMEG.

The metabolism of the N^6-cyclopropyl moiety has the potential to impart metabolic selectivity based on the enzymatic activity of various tissues. Although all radioactivity observed in tissues from ^{14}C-labeled PMEG can be assumed to represent PMEG and its phosphorylated metabolites, this is not necessarily the case for the material distributed by ^{14}C-labeled GS-9219. To identify the metabolites distributed to the liver by GS-9219, tissue extracts were analyzed by reverse-phase liquid chromatography comparing the radiolabeled peaks with authentic standards. Using this methodology, it was found that 100% of the extractable radioactivity in the liver and kidney 24 h after dose was associated with the dealkylation product PMEDAP (Fig. 4C and D), a molecule substantially less cytotoxic than either PMEG or cPrPMEDAP (Table 1; ref. 6). This is in contrast to circulating PBMCs, where PMEDAP was not detectable (levels <15 nmol/L) during pharmacokinetic studies (data not shown).

Taken together, the data from the comparative tissue distribution studies show that the prodrug moieties present in GS-9219 lead to a selective enrichment of PMEG in PBMCs and lymph nodes compared with other tissues, reducing the potential for off-target toxicities.

Selective depletion of lymphoid tissues in dogs receiving GS-9219. To compare the relative *in vivo* pharmacodynamic effects and toxicity of PMEG versus GS-9219, normal beagle dogs were given either compound by 30-min i.v. infusion daily for 5 days, GS-9219 dosed at 0.3 or 0.5 mg/kg, and PMEG dosed at 0.25 mg/kg. The 0.5 mg/kg dose of GS-9219 is approximately the molar equivalent of the 0.25 mg/kg dose of PMEG. Additional dogs received control infusions with vehicle. Lymphoid and nonlymphoid tissues were harvested for analysis 24 h after the last infusion. The most striking differences between the prodrug and PMEG were observed in lymphoid

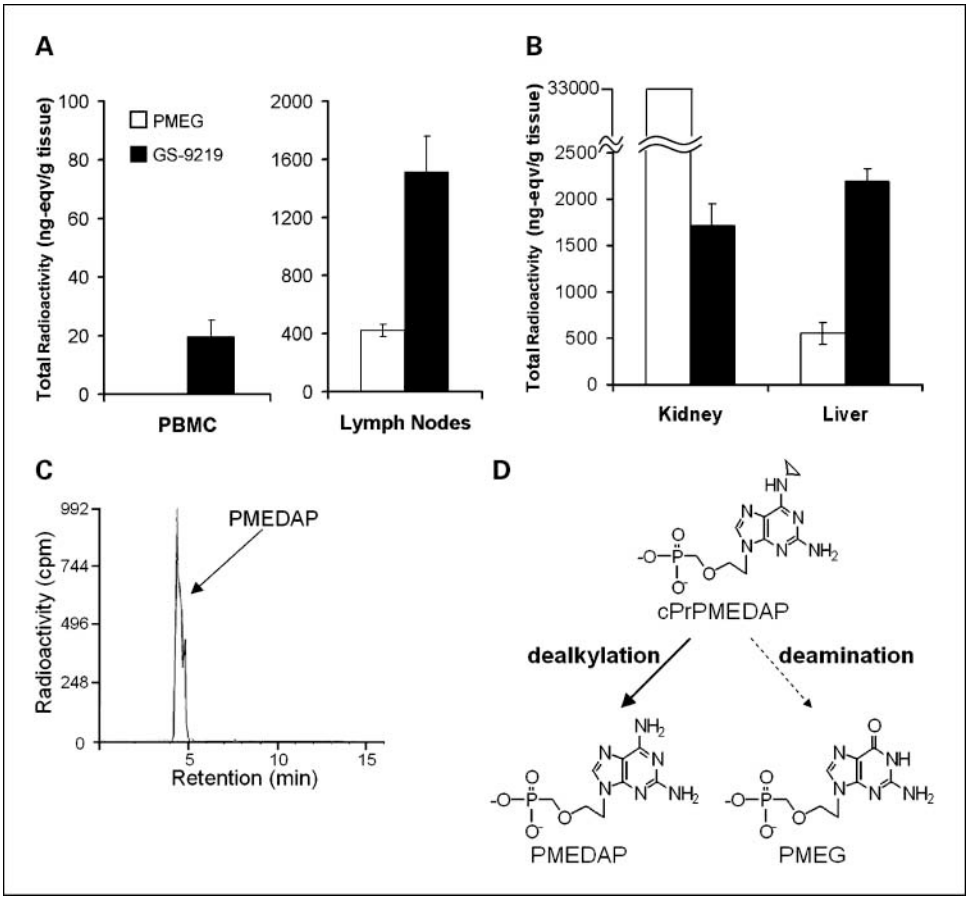

Fig. 4. Comparative analysis of tissue distribution and metabolism of GS-9219 and PMEG. *A,* comparison of the dose-normalized tissue distribution of [^{14}C]GS-9219 or [^{14}C]PMEG to hematopoietic cells and tissues. PBMCs and lymph nodes were harvested 24 h following administration of equimolar amounts of the two compounds. Columns, mean obtained from three animals; bars, SD. *B,* comparison of the dose-normalized tissue distribution of [^{14}C]GS-9219 or [^{14}C]PMEG to kidney and liver. Kidney and liver were harvested 24 h following administration of [^{14}C]GS-9219 or [^{14}C]PMEG. Columns, mean obtained from three animals; bars, SD. *C,* selective metabolism of the 6-amino prodrug moiety to PMEDAP in liver tissue. Radiolabel was extracted from liver tissue of dogs infused with [^{14}C]GS-9219. Radiolabeled peaks were separated by reverse-phase HPLC and compared with authentic standards to determine the identity of metabolites. *D,* based on the results obtained, dealkylation to PMEDAP is the predominant metabolic pathway in the liver.

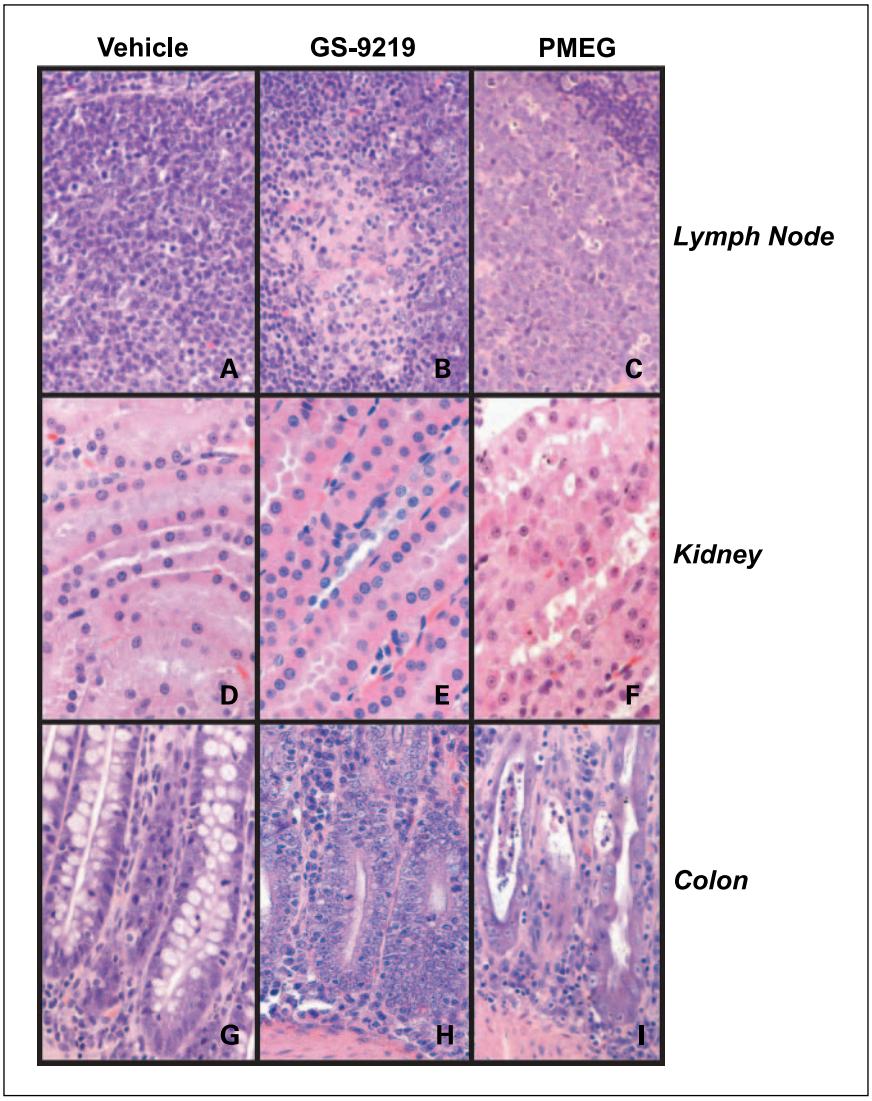

Fig. 5. Comparative toxicology analysis of GS-9219 and PMEG in normal beagle dogs. Normal beagle dogs received infusions with vehicle (*A, D,* and *G*), 0.5 mg/kg GS-9219 (*B, E,* and *H*), or 0.25 mg/kg PMEG (*C, F,* and *I*) on 5 consecutive days. Animals were sacrificed 24 h after the last infusion and representative organs were harvested and processed for histologic analysis by routine H&E staining. *A* to *C,* lymph node germinal centers. *D* to *F,* kidney (pars recta). *G* to *I,* colon (mucosa).

tissues and the major organs of PMEG toxicity, the kidney and gastrointestinal tract. Dogs infused with GS-9219 at doses of 0.3 mg/kg (data not shown) or 0.5 mg/kg (Fig. 5B) displayed pronounced depletion of lymphoid germinal centers, whereas PMEG had only a partial effect (Fig. 5C). Administration of PMEG resulted in significant cellular necrosis in the pars recta of the proximal tubules in the kidney (Fig. 5F) and in the gastrointestinal mucosa (Fig. 5I); by contrast, neither the 0.3 mg/kg (data not shown) nor the 0.5 mg/kg dose (Fig. 5E and H) of GS-9219 induced detectable changes in the kidney and only minimal to mild changes in the gastrointestinal tract. At these doses, GS-9219 produced no changes in the bone marrow (data not shown).

The results from comparative safety studies thus showed that GS-9219 has both significantly greater pharmacodynamic activity (depletion of germinal centers of lymphoid tissues) and significantly less off-target toxicity than PMEG. The results from these experiments with normal beagle dogs also suggested that there might be a therapeutic window for GS-9219 in hematologic malignancies because the compound selectively depleted replicating lymphocytes in lymphoid tissues while sparing other vital tissues, including the bone marrow and kidneys. Additional toxicology studies in normal beagle dogs showed that a single 30-min i.v. infusion of 1 mg/kg GS-9219 was well tolerated and induced significant depletion in the germinal centers of lymphoid follicles in lymph nodes as determined by routine H&E histology and by immunohistochemistry using an anti-Ki67 antibody (data not shown).

Single-dose, single-agent activity of GS-9219 in pet dogs with naturally occurring NHL. Based on the selective effects of GS-9219 on lymphoid tissues in normal beagle dogs, a preclinical proof-of-concept efficacy study was initiated in pet dogs with advanced-stage, spontaneously occurring NHL. The presentation and progression of NHL in dogs is similar to the disease in humans and is treated with similar agents (15). To evaluate the antitumor activity of GS-9219 in spontaneous NHL, five dogs with B-cell NHL were given a single 30-min i.v. infusion of GS-9219 (1 mg/kg) as monotherapy. Four of these dogs (dogs "A," "C," "D," and "E") were treatment naive, whereas the fifth dog (dog "B") had failed prior therapy with prednisone. The baseline characteristics of all dogs are summarized in Supplementary Table S1.

The GS-9219 infusion was well tolerated in all animals. Antitumor activity was evaluated based on reduction in tumor size determined by the sums of the longest diameter of the affected nodes using Response Evaluation Criteria in Solid Tumors adopted for use in Veterinary Oncology (16, 17). As shown in Supplementary Table S2, a single 30-min infusion induced major responses (partial or complete) in all five dogs as assessed 5 to 7 days after treatment. Specifically, three partial responses (dogs A, B, and C) and two complete responses (dogs D and E) were observed. To assess the effect of GS-9219 on tumor cell proliferation rate, one of the dogs was also evaluated before and after dose by PET/CT using FLT as the tracer. Imaging with this tracer has been shown to correlate with early response assessment in humans with NHL (18). The PET/CT scan results depicted in Fig. 6 illustrate significant reduction in tumor cell proliferation at each site (popliteal, mesenteric, mediastinal, prescapular, and submandibular lymph nodes). Taken together, these results show that GS-9219 has significant single-agent activity in dogs with advanced-stage, spontaneously occurring NHL.

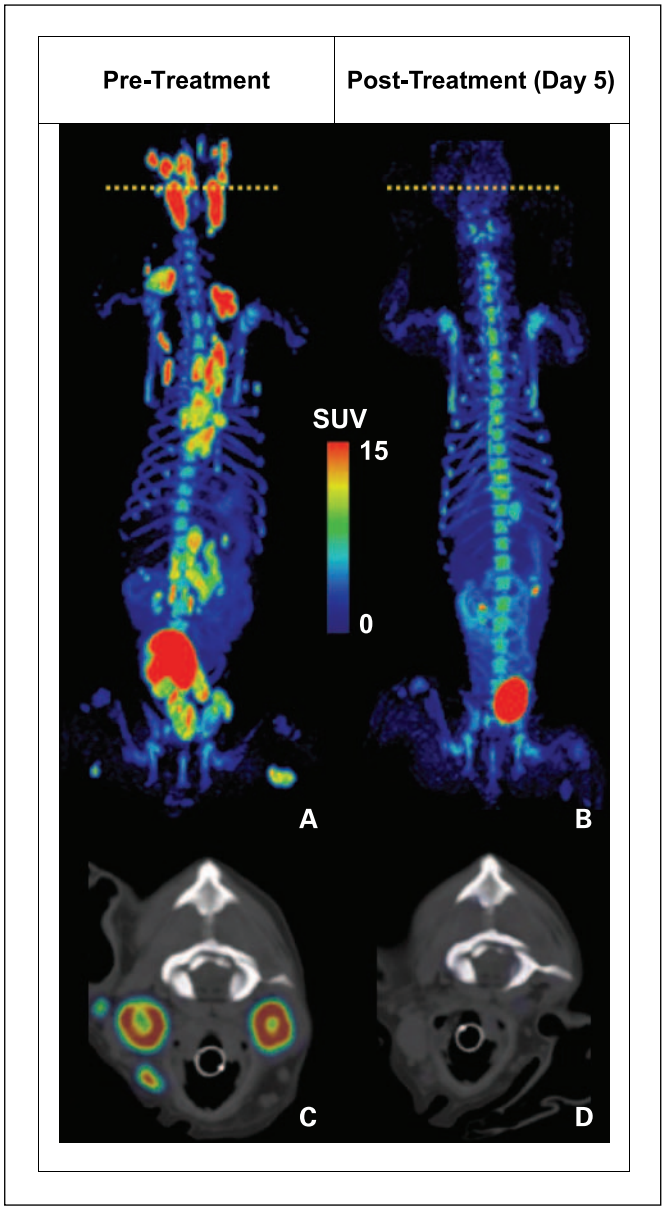

Fig. 6. PET/CT scan before and 5 d after a single 1 mg/kg (0.82 mg/kg free base) dose of GS-9219 in a dog with refractory NHL (dog B). The cell proliferation marker FLT was used to assess proliferative response to the GS-9219 therapy. The comparison between the whole-body PET scan before therapy (*A*) and 5 d after therapy (*B*) shows significant proliferative response in affected lymphoid tissues (popliteal, mesenteric, mediastinal, prescapular, and submandibular lymph nodes). Note that the signal in the urinary bladder and renal calyces is normal and represents urinary excretion of the tracer. Low-level signal present in the vertebral bone marrow and the gastrointestinal tract reflects background uptake of tracer in the proliferating cell populations in these tissues. In *C* and *D*, the axial PET/CT pretreatment and posttreatment scans are shown clearly indicating proceeding biological response in comparison with the anatomic response. The axial views are displayed at the position of the yellow dotted lines on the whole-body PET scans and represent the level of the mandibular lymph nodes.

Discussion

Acyclic nucleotide analogues do not require the often rate-limiting first phosphorylation step to produce the active triphosphate species. Members of this compound class display a broad spectrum of activity against a range of DNA viruses and retroviruses (19). In addition, several of the acyclic nucleotides exhibit antiproliferative activity in eukaryotic cells. The guanine derivative PMEG is the most cytotoxic of the acyclic nucleoside phosphonate analogues studied (20). Its active metabolite, PMEGpp, is a potent inhibitor of DNA polymerases α, δ, and ε (21, 22), enzymes known to participate in eukaryotic DNA replication and/or DNA repair. PMEGpp is efficiently recognized as an alternative substrate by these polymerases (2, 23), resulting in its incorporation into nascent DNA chains and termination of DNA synthesis. This leads to the arrest of cell division in S phase with subsequent induction of apoptosis.

Consistent with its potent *in vitro* activities, PMEG is the most effective acyclic nucleoside phosphonate in murine models of cancer, inhibiting the growth of both P388 leukemia cells and B16 melanoma cells (3). However, the therapeutic utility of PMEG is limited by its toxicity, which was originally observed in these pharmacologic models (3). Our approach, presented in this report, has been to design a double prodrug version of PMEG. The selected compound, GS-9219, is hydrolyzed intracellularly to cPrPMEDAP, subsequently deaminated to PMEG, and finally phosphorylated to PMEGpp. GS-9219 was selected because of its antiproliferative activity *in vitro* and its ability to effectively deliver PMEG metabolites into PBMCs *in vivo* while maintaining low plasma levels of potentially toxic PMEG. The small amount of cPrPMEDAP in plasma seems to be released from tissues and not formed by cleavage in the plasma, based on the delayed time to maximum cPrPMEDAP concentration and the high stability of GS-9219 in canine plasma (data not shown). In contrast to efficient intracellular metabolism of cPrPMEDAP, its deamination does not readily occur in plasma, minimizing the systemic exposure to PMEG.

Pharmacokinetic studies show that the short systemic exposure to GS-9219 is sufficient to load lymphoid cells with persistent and pharmacologically effective levels of PMEGpp. The double prodrug strategy increases the selectivity of PMEG by (*a*) more efficiently loading target lymphoid cells and tissues, (*b*) reducing distribution to sites of potential dose-limiting toxicity (kidney), and (*c*) selective metabolism of the

N^6 moiety in different tissues. Selective metabolism of the N^6 moiety includes deamination of cPrPMEDAP in lymphocytes, resulting in subsequent formation of the active species PMEGpp, and dealkylation in the liver followed by renal excretion of the less cytotoxic nucleotide PMEDAP. The accumulation of GS-9219 metabolites in lymphoid tissues is likely a consequence of a highly active multistep catabolic pathway leading to the intracellular generation of PMEGpp. In contrast, this pathway does not seem to operate efficiently in plasma or liver, resulting in improved selectivity. As PMEG is readily accumulated in kidney via its interaction with renal uptake transporters expressed in proximal tubules (24), the lack of systemic exposure to PMEG in animals dosed with GS-9219 is likely the major factor in reducing the nephrotoxicity of this prodrug. The mechanism of dealkylation of cPrPMEDAP to PMEDAP has not been identified, but cytochrome *P*450 enzymes have been noted to catalyze this reaction on molecules of similar chemical structure (25).

GS-9219 has substantial antiproliferative activity against activated lymphocytes and tumor cell lines of hematopoietic origin. The ability of GS-9219 to inhibit the proliferation of cell lines of nonhematopoietic origin was also tested. In general, solid tumor cell lines seemed less sensitive to GS-9219 than cell lines of hematopoietic origin (data not shown), underscoring the compound selectivity. Given the weak cytotoxicity of GS-9219 in quiescent cells, combination of GS-9219 with agents and modalities that initiate DNA repair may have clinical relevance in the treatment of certain malignancies.

GS-9219 depleted the germinal centers in lymphoid tissues of normal beagle dogs at doses and regimens that produce only minimal to mild changes in the gastrointestinal tract and no effects on the bone marrow or kidney. In addition, GS-9219 displayed significant *in vivo* efficacy in five dogs with spontaneously occurring, advanced-stage NHL after a single i.v. administration. Of note, reduction in tumor burden occurred with either none or only low-grade (grade 1 or 2) adverse events (data not shown). We continue to evaluate the nonclinical efficacy of GS-9219 in dogs with hematologic malignancies, including NHL. Given the promising preclinical attributes of GS-9219, we have initiated a human phase I/II study of GS-9219 in patients with hematologic malignancies. The results of these studies will be presented when completed.

References

1. Jemal A, Siegel R, Ward E, et al. Cancer statistics, 2006. CA Cancer J Clin 2006;56:106–30.
2. Kramata P, Downey KM, Paborsky LR. Incorporation and excision of 9-(2-phosphonylmethoxyethyl)guanine (PMEG) by DNA polymerase δ and ε *in vitro*. J Biol Chem 1998;273:21966–71.
3. Rose WC, Crosswell AR, Bronson JJ, Martin JC. *In vivo* antitumor activity of 9-[(2-phosphonylmethoxy)ethyl]-guanine and related phosphonate nucleotide analogues. J Natl Cancer Inst 1990;82:510–2.
4. Valerianova M, Votruba I, Holy A, Mandys V, Otova B. Antitumour activity of N^6-substituted PMEDAP derivatives against T-cell lymphoma. Anticancer Res 2001;21:2057–64.
5. Naesens L, Hatse S, Segers C, et al. 9-(2-Phosphonylmethoxyethyl)-N^6-cyclopropyl-2,6-diaminopurine: a novel prodrug of 9-(2-phosphonylmethoxyethyl)guanine with improved antitumor efficacy and selectivity in choriocarcinoma-bearing rats. Oncol Res 1999;11:195–203.
6. Hatse S, Naesens L, De Clercq E, Balzarini J. N^6-cyclopropyl-PMEDAP: a novel derivative of 9-(2-phosphonylmethoxyethyl)-2,6-diaminopurine (PMEDAP) with distinct metabolic, antiproliferative, and differentiation-inducing properties. Biochem Pharmacol 1999;58:311–23.
7. Compton ML, Toole JJ, Paborsky LR. 9-(2-Phosphonylmethoxyethyl)-N^6-cyclopropyl-2,6-diaminopurine (cpr-PMEDAP) as a prodrug of 9-(2-phosphonylmethoxyethyl)guanine (PMEG). Biochem Pharmacol 1999;58:709–14.
8. Wetzler LM, HoY, Reiser H. Neisserial porins induce B lymphocytes to express costimulatory B7-2 molecules and to proliferate. J Exp Med 1996;183:1151–9.
9. Vela JE, Olson LY, Huang A, Fridland A, Ray AS. Simultaneous quantitation of the nucleotide analog adefovir, its phosphorylated anabolites and 2′-deoxyadenosine triphosphate by ion-pairing LC/MS/MS. J Chromatogr B Analyt Technol Biomed Life Sci 2007;848:335–43.
10. Vail DM. Veterinary co-operative oncology group-common terminology criteria for adverse events (VCOG-CTCAE) following chemotherapy or biological antineoplastic therapy in dogs and cats v1.0. Vet Compar Oncol 2004;2:194–213.
11. Birkus G, Wang R, Liu X, et al. Cathepsin A is a major hydrolase catalyzing the intracellular hydrolysis of the antiretroviral nucleotide phosphonoamidate prodrugs GS-7340 and GS-9131. Antimicrob Agents Chemother 2007;51:1–7.
12. Schinkmanova M, Votruba I, Holy A. N^6-methyl-AMP aminohydrolase activates N^6-substituted purine acyclic nucleoside phosphonates. Biochem Pharmacol 2006;71:1370–6.
13. Parker WB, Secrist JA III, Waud WR. Purine nucleoside antimetabolites in development for the treatment of cancer. Curr Opin Investig Drugs 2004;5:592–6.
14. Haas D, Ribaudo H, Kim R, et al. A common CYP2B6 variant is associated with efavirenz pharmacokinetics and central nervous system side effects: AACTG Study NWCS214 [abstract 133]. In: 11th Conference on Retroviruses and Opportunistic Infections, San Francisco, California.
15. Vail DM, Thamm DH. Spontaneously occurring tumors in companion animals as models for drug development. In: Teicher BA, Andrews PA, editors. Cancer drug discovery and development: anticancer drug development guide: preclinical screening, clinical trials, and approval. Totowa (NJ): Humana Press, Inc.; p. 259–84.
16. Therasse P, Arbuck SG, Eisenhauer EA, et al. New guidelines to evaluate the response to treatment in solid tumors. European Organization for Research and Treatment of Cancer, National Cancer Institute of the United States, National Cancer Institute of Canada. J Natl Cancer Inst 2000;92:205–16.
17. Therasse P, Eisenhauer EA, Verweij J. RECIST revisited: a review of validation studies on tumour assessment. Eur J Cancer 2006;42:1031–9.
18. Herrmann K, Wieder HA, Buck AK, et al. Early response assessment using 3′-deoxy-3′-[18F]fluorothymidine-positron emission tomography in high-grade non-Hodgkin's lymphoma. Clin Cancer Res 2007;13:3552–8.
19. De Clercq E, Holy A. Acyclic nucleoside phosphonates: a key class of antiviral drugs. Nat Rev Drug Discov 2005;4:928–40.
20. Franek F, Holy A, Votruba I, Eckschlager T. Acyclic nucleotide analogues suppress growth and induce apoptosis in human leukemia cell lines. Int J Oncol 1999;14:745–52.
21. Pisarev VM, Lee S-H, Connelly MC, Fridland A. Intracellular metabolism and action of acyclic nucleoside phosphonates on DNA replication. Mol Pharmacol 1997;52:63–8.
22. Cundy KC. Pharmacokinetics of PMPA in a 14-day intravenous infusion toxicity study in cynomolgus monkeys (a report on analysis of plasma concentration data from toxicity study #96-Tox-1278-002). Report no. 96-TOX-1278-002-PK. Foster City (CA): Gilead Sciences, Inc.; 1996.
23. Cihlar T, Chen MS. Incorporation of selected nucleoside phosphonates and anti-human immunodeficiency virus nucleotide analogues into DNA by human DNA polymerases α, β and γ. Antivir Chem Chemother 1997;8:187–95.
24. Cihlar T, Lin DC, Pritchard JB, et al. The antiviral nucleotide analogs cidofovir and adefovir are novel substrates for human and rat renal organic anion transporter 1. Mol Pharmacol 1999;56:570–80.
25. Cerny MA, Hanzlik RP. Cytochrome *P*450-catalyzed oxidation of *N*-benzyl-*N*-cyclopropylamine generates both cyclopropanone hydrate and 3-hydroxypropionaldehyde via hydrogen abstraction, not single electron transfer. J Am Chem Soc 2006;128:3346–54.